Metallomics

Accepted Manuscript

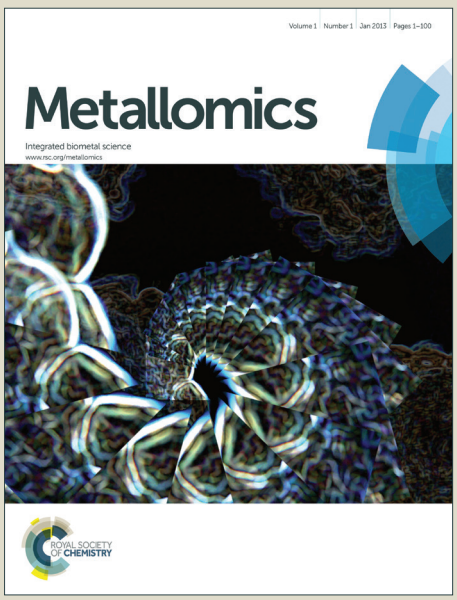

ROYAL SOCIETY OF CHEMISTRY

www.rsc.org/metallomics

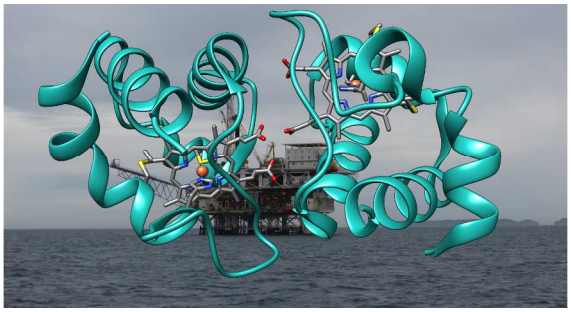

The molecular structure of the electron-transfer protein cytochrome c_{552} from a cold-adapted, hydrocarbon-degrading marine bacterium is reported (PDB: 4O1W).

The structure of ferricytochrome c_{552} from the psychrophilic marine bacterium *Colwellia psychrerythraea* 34H

Paul B. Harvilla,[a,b] Holly N. Wolcott,[b] and John S. Magyar[a,*]

[a]Department of Chemistry, Barnard College, Columbia University, 3009 Broadway, New York, NY 10027
[b]Department of Biochemistry and Molecular Biophysics, Columbia University, New York, NY 10032

Abstract

Approximately 40% of all proteins are metalloproteins, and approximately 80% of Earth's ecosystems are at temperatures ≤ 5 °C, including 90% of the global ocean. Thus, an essential aspect of marine metallobiochemistry is an understanding of the structure, dynamics, and mechanisms of cold adaptation of metalloproteins from marine microorganisms. Here, the molecular structure of the electron-transfer protein cytochrome c_{552} from the psychrophilic marine bacterium *Colwellia psychrerythraea* 34H has been determined by X-ray crystallography (PDB: 4O1W). The structure is highly superimposable with that of the homologous cytochrome from the mesophile *Marinobacter hydrocarbonoclasticus*. Based on structural analysis and comparison of psychrophilic, psychrotolerant, and mesophilic sequences, a methionine-based ligand-substitution mechanism for psychrophilic protein stabilization is proposed.

Introduction

Since the discovery of life at geothermal features, both marine and terrestrial, thermophilic organisms and the proteins they produce have received much attention from researchers. Often unrecognized is the fact that most of Earth's ecosystems (~80%) are permanently at temperatures ≤ 5 °C. These ecosystems include the global ocean below 1000 m in addition to polar and alpine regions. Moreover, there is an amazing diversity of life that not only thrives in these cold environments but also, in many cases, requires low temperatures for survival.[1-2] These psychrophilic ("cold-loving") organisms play major roles in global nutrient cycling, as well as in bioremediation of both anthropogenic oil spills and natural petroleum seeps.

The importance of psychrophilic microorganisms is particularly clear in the aftermath of the catastrophic blowout of BP's *Deepwater Horizon*/Macondo MC252 well in the Gulf of Mexico in 2010. In addition to the tragic loss of 11 workers in the resulting fire and explosions, 780 million liters (4.9 million barrels) of oil were spilled over 84 days.[3-4] A particular challenge for the cleanup was the fact that the spill occurred at 1500 m depth. Beyond the well-documented engineering challenges and oil plume dynamics associated with the great depth, an important environmental consideration was the fact that the Gulf of Mexico below 700 m is continually 2-5 °C. Analysis during and after the spill has revealed that the natural microbial consortia involved in hydrocarbon

bioremediation in the cold, deep water of the Gulf of Mexico are different from those in surface waters or in coastal sediments.[5-14]

Among the primary groups of hydrocarbonoclastic microorganisms found in deep, cold Gulf water samples after the Macondo blowout were species of *Colwellia*.[5-6] Additional studies have confirmed the ability of *Colwellia* sp. isolated from the spill environment to degrade hydrocarbons effectively.[7, 9] Most *Colwellia* observed to date are obligately psychrophilic bacteria; that is, they require temperatures below 10 °C for growth. The type strain *Colwellia psychrerythraea* 34H, the genome of which has been sequenced, was isolated from Arctic marine sediments.[15]

Incidents such as the BP/*Deepwater Horizon* oil spill emphasize how little is still known of psychrophilic microbiology. Even less is known about the biological inorganic chemistry of these organisms. A persistent question is how cellular processes such as electron transfer, energy storage, and metal ion homeostasis occur with reasonable rates at decreased temperatures. Investigations of psychrophilic bioinorganic chemistry are essential to understanding the roles of psychrophilic and psychrotolerant microorganisms[16-17] in global biogeochemical cycles and in bioremediation.

As a window into elucidating what molecular adaptations must take place to support the psychrophilic lifestyle, we have been studying the electron transfer

metalloprotein cytochrome c_{552} from *Colwellia psychrerythraea* 34H.[18-19] The protein sequence is provided as Figure S1 (Supporting Information). Here, we report the first X-ray crystal structure of a *c*-type cytochrome from a psychrophilic microorganism. We compare this structure with published structures from homologous mesophilic cytochromes and highlight features that may be important psychrophilic adaptations. We suggest future work to further elucidate molecular mechanisms of psychrophilicity, with a particular emphasis on metal–ligand substitution processes in cytochrome *c*.

Results and Discussion

The structure of cytochrome c_{552} from *C. psychrerythraea* 34H (*Cp*cyt c_{552}) was determined to 2.00 Å resolution using synchrotron radiation (Figure 1, Table S1, PDB: 4O1W). The *Cp*cyt c_{552} structure is highly superimposable with the structure of cytochrome c_{552} from the mesophilic marine bacterium *Marinobacter hydrocarbonoclasticus*, formerly known as *Pseudomonas nautica* (*Mh*cyt c_{552}, PDB: 1CNO).[20-21] Figure 2 shows the superposition of single monomers of *Mh*cyt c_{552} and *Cp*cyt c_{552}. The high structural similarity combined with only moderate sequence similarity (57%) makes this pair of proteins an excellent system for investigating the molecular basis of specific psychrophilic adaptations.

*Cp*cyt c_{552} forms a dimer in the solid state (Figure 1); there are six monomers in the asymmetric unit, grouped into three dimer pairs (Figure S2). As in the case of *Mh*cyt c_{552}, the structure of the *Cp*cyt c_{552} dimer is extremely similar to that of

two-heme cytochromes such as cytochrome c_4 from *Pseudomonas stutzerii* (PDB: 1ETP).[20, 22] Figure S3 shows the superposition of the three structures. Both size exclusion chromatography and analytical ultracentrifugation indicate that *Cp*cyt c_{552} is a dimer in solution as well as in the solid state. The electron-transfer partner of *Cp*cyt c_{552} is not yet known; but the structure is consistent with the idea that *Cp*cyt c_{552} acts as an electron shuttle to cytochrome *c* peroxidase and/or nitrous oxide reductase, as reported for *Mh*cyt c_{552}.[20, 23]

As shown in Figure 3, the dimer interface is dominated by interactions between the propionate groups of the two hemes, along with hydrogen bonds from the heme propionates to Tyr39, Lys42, Gln43 and Arg52. As observed by Brown *et al.* for *Mh*cyt c_{552}, the closeness of the propionate oxygens between the two monomer units (2.537 Å in *Cp*cyt c_{552}) indicates that one of the propionate oxygens must be protonated and hydrogen bonded to the propionate oxygen of the heme in the other monomer. Otherwise, the interaction between those two oxygens would be highly repulsive.[20]

The iron is axially coordinated to His18 through nitrogen and to Met57 via sulfur, as is typical for cytochrome c_{552}. Iron–ligand distances are consistent with assignment as low-spin Fe(III). The heme in each monomer exhibits moderate ruffling, as is expected for *c*-type cytochromes.[24-26]

Of particular interest in the amino acid sequence of *Cp*cyt c_{552} is the relatively high number of methionine residues (six), most of which are highly conserved in sequences from psychrophilic bacteria. The structure of *Cp*cyt c_{552} reveals that although Met57 is the axial methionine, upon ligand dissociation a minor structural change would permit Met60 to ligate the heme iron in place of Met57 (Figure S4). In fact, it appears practical for any one of five of the six methionines to misligate the heme upon partial protein unfolding: Met57, Met60, Met62, Met69, and Met 79. (Met13 is adjacent to the cysteines (Cys14, Cys17) that are covalently bound to the heme vinyl groups and is thus constrained from iron coordination.)

We propose that as the protein unfolds, perhaps with temperature fluctuations in its marine environment, the native methionine (Met57) dissociates from the heme iron. Because the overall protein is highly flexible (Figure S5), more so than its mesophilic counterparts, the dissociation of Met57 has the potential to lead rapidly to full denaturation. If the protein unfolds completely, it may get trapped in a deep well on the protein folding energy landscape from which it cannot escape. However, heme ligation by a nearby methionine residue may keep the protein from unfolding completely. This heme–methionine misligation would keep the protein in shallow energy minima on the folding landscape, allowing it the opportunity to refold and regain both native structure and native ligation. The heme misligation keeps the protein minimally frustrated,[27-28] increasing the barrier to irreversible denaturation.

Such a mechanism, comparable to heme misligation by histidine in mitochondrial cytochromes *c* during the protein folding process,[29-30] could account in part for the surprising stability we have observed for *Cp*cyt c_{552}.[18] In the mitochondrial cytochromes, it is now well accepted that the heme works as a built-in folding chaperone, with heme misligation by His26 and His33 expediting protein folding by supporting the formation of native contacts.[30-31] It has long been proposed that psychrophilic proteins have greater flexibility so that protein dynamics at low temperatures can be equivalent to the dynamics of mesophilic proteins at room temperature.[32] Questions remain, however, whether this flexibility is global or is localized to particular areas of a protein, and also how this increased flexibility might impact protein stability. Little attention has been paid to the role that metal–ligand binding might play in modulating protein stability or flexibility.

The question arises why psychrophilic marine bacteria might use methionine as a stabilizing ligand instead of using histidines as mesophilic mitochondrial cytochromes do. We suggest that the answer may lie in the temperature dependence of acid-base equilibria. As noted by E. J. King in 1965, "Our devotion to values of K_a at 25 °[C] must not blind us to the fact that the relative strength of two acids is altered by a change in temperature."[33] There is significant variability in the degree to which temperature changes affect pK_a values, a fact too often overlooked. The pK_a of imidazole, the side chain of the amino acid histidine, has a small but significant temperature dependence (dpK_a/dT = –

0.020).[34] Importantly, this change takes the pK_a of imidazole from 6.95 at 25 °C to > 7.4 at 0-5 °C,[35-36] the temperatures at which psychrophilic marine microorganisms such as *Colwellia* are living. Thus, at the pH of the cell, histidine will be found commonly in its protonated state at 0-5 °C, in contrast to its deprotonated condition at 25 °C or higher. The increased protonation of histidine at low temperatures, and thus its unsuitability as a metal-binding ligand, could have led to the evolutionary use of methionine rather than histidine as a stabilizing ligand in psychrophilic microorganisms. Methionine metal binding is through a thioether sulfur, which cannot be protonated under cellular conditions.

Met57 (the native axial methionine), Met60, and Met62 are highly conserved in cytochromes from psychrophilic and psychrotolerant bacteria but not in those from mesophilic bacteria (Figure S6). This observation is consistent with the idea that these methionines play a role in stabilizing the protein structure in psychrophilic cyt c_{552} in ways that are unnecessary in mesophilic cyt c_{552}.

In the crystal structure reported here, there are six monomers in the asymmetric unit, arranged in three dimer-pairs. Using MatchMaker in UCSF Chimera,[37] we superimposed the structures of each of the dimer pairs to look for variations (Figure S7). Substantial differences in the orientation of the methionine side chain exist for both Met60 and Met62 in different copies of the dimer in the asymmetric unit. These differences in the solid state structure may result from a variety of factors, including crystal packing. They suggest, however, a degree of

flexibility in these amino acids consistent with ligand substitution reactions. The crystallographic B-factors for these amino acids (26.7-48.3 $Å^2$) are higher than the average for the structure (25.20 $Å^2$), consistent with greater structural dynamics (Figure S5).[38] (By comparison, the B-factors for the iron-bound axial Met57 are much lower, 15.1-25.6 $Å^2$.)

Of note, little to no interchain positional variation was observed for Met69 and Met79. Met69 and Met79 are much less well conserved and are frequently substituted by leucine or isoleucine even in psychrophilic proteins, suggesting that the hydrophobicity of the residue is more important than its metal-binding capabilities in those positions.

The protein crystal structure reported here provides valuable insights into the potential role of methionine in accounting for the surprising stability of *Cp*cyt c_{552}. In previous work, we reported that *Cp*cyt c_{552} is more stable (*i.e.*, it has a higher midpoint temperature of unfolding) than expected for a flexible, psychrophilic protein.[18] The structural parameters reported here are consistent with a flexible protein but also suggest a possible mechanism for protein stabilization based on ligand substitution processes, specifically binding of heme iron by non-native methionine ligands. Analysis of the *Cp*cyt c_{552} molecular structure coupled with sequence alignments of related psychrophilic, psychrotolerant, and mesophilic proteins points to Met60 and Met62 as the most likely candidates for a role in

heme misligation. We are beginning further spectroscopic, structural, site-directed mutagenesis, and computational studies to investigate this prediction.

Experimental

*Cp*cyt c_{552} was overexpressed in *Escherichia coli* BL21(DE3)-Star and purified by cation exchange chromatography as previously reported.[18] The mass of *Cp*cyt c_{552} was confirmed by MALDI-TOF mass spectrometry (Scripps Center for Mass Spectrometry, La Jolla, CA); calculated mass 8832 Da, measured m/z 8834. Initial crystal hits were obtained for *Cp*cyt c_{552} using a Mosquito protein crystallization robot (TTP Labtech) and the JCSG Core IV screen (Qiagen). Crystals were further optimized to diffraction quality in a condition containing 0.2 M lithium sulfate, 28-30% PEG 4000, 50 mM Tris pH 9.0, and 5% trehalose. Diffraction experiments were conducted on beamline X4C at the National Synchrotron Light Source (NSLS) at Brookhaven National Laboratory. Owing to the large, planar nature of the crystals obtained, only crystals grown in 5% cryo-additive displayed favorable freezing properties. One crystal diffracted to 2.01 Å with reasonable mosaicity allowing for structure determination. The data were processed in HKL2000, and phases were obtained using molecular replacement in the program Phaser. Refinement was carried out using Refmac with manual model building in Coot, and all residues fell in the favorable region of the Ramachandran plot (Figure S8). The structure has been deposited in the Protein Data Bank (www.pdb.org) with PDB code 4O1W.

UV-visible absorption spectra were obtained using a Varian Cary 5000 UV-vis-NIR spectrophotometer. The spectra are as described previously.[18] The oligomerization state of *Cp*cyt c_{552} in solution was determined by analytical size exclusion chromatography with a Superdex 75 10/300 GL column and an ÄKTApurifier (GE Healthcare), calibrated with Low Molecular Weight Calibration Standards (GE Healthcare).

Conclusion

The secondary, tertiary, and quaternary structure of *Cp*cyt c_{552}, as determined by X-ray crystallography, are nearly identical to known cytochrome structures, low to moderate sequence similarity notwithstanding. This experimental demonstration of structural similarity confirms *Cp*cyt c_{552} as an excellent model system for studies of molecular mechanisms of psychrophilicity. Like its mesophilic homologue from *M. hydrocarbonoclasticus*, *Cp*cyt c_{552} crystallizes as a dimer reminiscent of two-heme cytochromes such as cytochrome c_4 from *Pseudomonas stutzerii*. Positioning of methionine residues in *Cp*cyt c_{552} is consistent with a proposal for heme–methionine misligation as a stabilization mechanism. Structural thermal parameters (B-factors) and differential orientation of the Met60 and Met62 side chains in multiple copies of the protein within the asymmetric unit are consistent with a dynamic role for these residues. This structural study provides insights into mechanisms of psychrophilicity in marine metalloproteins and suggests additional experiments to further elucidate these mechanisms.

Acknowledgments

We gratefully acknowledge funding from the National Science Foundation (CHE-1308170, MRI-R^2 CHE-0959177, ARI-R^2 CHE-0961709), a Camille and Henry Dreyfus Foundation Faculty Start-Up Award, a Barnard College Presidential Research Award, the New York Division of Science, Technology, and Innovation (NYSTAR), the Columbia NSF NSEC: Center for Electron Transport in Molecular Nanostructures (CHE-0117752 and CHE-0641523), the NIH Training Program in Molecular Biophysics at Columbia (PBH, HNW) (T32 GM008281), and Barnard College. This work was performed in part using facilities of the New York Structural Biology Center, including Beamline X4C at NSLS, supported by the State of New York. We thank Art Palmer and Lawrence Shapiro for their support of this project and Linda Thöny-Meyer for generously making the pEC86 plasmid available. Molecular graphics and analyses were performed with the UCSF Chimera package, developed by the Resource for Biocomputing, Visualization, and Informatics at the University of California, San Francisco (supported by NIGMS P41-GM103311).

References

1. B. A. Methé, K. E. Nelson, C. M. Fraser, *Trends Microbiol.* 2004, **12,** 532-534.

2. G. Feller, C. Gerday, *Nat. Rev. Microbiol.* 2003, **1,** 200-208.

3. R. M. Atlas, T. C. Hazen, *Environ. Sci. & Technol.* 2011, **45,** 6709-6715.

4. The Federal Interagency Solutions Group: Oil Budget Calculator Science and Engineering Team. 2010. *Oil Budget Calculator Technical Documentation*. http://www.restorethegulf.gov/sites/default/files/documents/pdf/OilBudgetCalc_Full_HQ-Print_111110.pdf (accessed January 25, 2014).

5. M. C. Redmond, D. L. Valentine, *Proc. Natl. Acad. Sci. USA* 2011, **109,** 20292-20297.

6. M. C. Redmond, D. V. Valentine, A. L. Sessions, *Appl. Environ. Microbiol.* 2010, **76,** 6412-6422.

7. T. Gutierrez, D. R. Singleton, D. Berry, T. Yang, M. D. Aitken, A. Teske, *ISME J.* 2013, **7,** 2091-2104.

8. E. A. Dubinsky, M. E. Conrad, R. Chakraborty, M. Bill, S. E. Borglin, J. T. Hollibaugh, O. U. Mason, Y. M. Piceno, F. C. Reid, W. T. Stringfellow, L. M. Tom, T. C. Hazen, G. L. Andersen, *Environ. Sci. & Technol.* 2013, **47,** 10860-10867.

9. J. Bælum, S. Borglin, R. Chakraborty, J. L. Fortney, R. Lamendella, O. U. Mason, M. Auer, M. Zemla, M. Bill, M. E. Conrad, S. A. Malfatti, S. G. Tringe, H.-Y. Holman, T. C. Hazen, J. K. Jansson, *Environ. Microbiol.* 2012, **14,** 2405-2416.

10. R. Chakraborty, S. E. Borglin, E. A. Dubinsky, G. L. Andersen, T. C. Hazen, *Front. Microbiol.* 2012, **3,** 357.

11. B. R. Edwards, C. M. Reddy, R. Camilli, C. A. Carmichael, K. Longnecker, B. A. S. Van Mooy, *Environ. Res. Lett.* 2011, **6,** 035301.

12. R. Camilli, C. M. Reddy, D. R. Yoerger, B. A. S. Van Mooy, M. V. Jakuba, J. C. Kinsey, C. P. McIntyre, S. P. Sylva, J. V. Maloney, *Science* 2010, **330,** 201-204.

13. J. E. Kostka, O. Prakash, W. A. Overholt, S. J. Green, G. Freyer, A. Canion, J. Delgardio, N. Norton, T. C. Hazen, M. Huettel, *Appl. Environ. Microbiol.* 2011, **77,** 7962-7974.

14. T. C. Hazen, E. A. Dubinsky, T. Z. DeSantis, G. L. Andersen, Y. M. Piceno, N. Singh, J. K. Jansson, A. Probst, S. E. Borglin, J. L. Fortney, W. T. Stringfellow, M. Bill, M. E. Conrad, L. M. Tom, K. L. Chavarria, T. R. Alusi, R. Lamendella, D. C. Joyner, C. Spier, J. Baelum, M. Auer, M. L. Zemla, R. Chakraborty, E. L. Sonnenthal, P. D'haeseleer, H. N. Holman, S. Osman, Z. Lu, J. D. Van Nostrand, Y. Deng, J. Zhou, O. U. Mason, *Science* 2010, **330,** 204-208.

15. B. A. Methé, K. E. Nelson, J. W. Deming, B. Momen, E. Melamud, X. Zhang, J. Moult, R. Madupu, W. C. Nelson, R. J. Dodson, L. M. Brinkac, S. C. Daugherty, A. S. Durkin, R. T. DeBoy, J. F. Kolonay, S. A. Sullivan, L. Zhou, T. M. Davidsen, M. Wu, A. L. Huston, M. Lewis, B. Weaver, J. F. Weidman, H. Khouri, T. R. Utterback, T. V. Feldblyum, C. M. Fraser, *Proc. Natl. Acad. Sci. USA* 2005, **102,** 10913-10918.

16. R. Y. Morita, *Bacteriolog. Rev.* 1975, **39,** 144-167.

17. E. Helmke, H. Weyland, *Cell. Mol. Biol.* 2004, **50,** 553-561.

18. V. F. Oswald, W. Chen, P. B. Harvilla, J. S. Magyar, *J. Inorg. Biochem.* 2014, **131,** 76-78.

19. O. M. Sokolovskaya, J. S. Magyar, M. C. Buzzeo, *J. Phys. Chem. C* submitted.

20. K. Brown, D. Nurizzo, S. Besson, W. Shepard, J. Moura, I. Moura, M. Tegoni, C. Cambillau, *J. Mol. Biol.* 1999, **289,** 1017-1028.

21. C. Spröer, E. Lang, P. Hobeck, J. Burghardt, E. Stackebrandt, B. J. Tindall, *Int. J. Syst. Bacteriol.* 1998, **48,** 1445-1448.

22. A. Kadziola, S. Larsen, *Structure* 1997, **5,** 203-216.

23. S. Dell'Acqua, S. R. Pauleta, E. Monzani, A. S. Pereira, L. Casella, J. J. G. Moura, I. Moura, *Biochemistry* 2008, **47,** 10852-10862.

24. J.-G. Ma, M. Laberge, X.-Z. Song, W. Jentzen, S.-L. Jia, J. Zhang, J. M. Vanderkooi, J. A. Shelnutt, *Biochemistry* 1998, **37,** 5118-5128.

25. M. Can, J. Krucinska, G. Zoppellaro, N. H. Andersen, J. E. Wedekind, H.-P. Hersleth, K. K. Andersson, K. L. Bren, *ChemBioChem* 2013, **2013,** 1828-1838.

26. M. Can, G. Zoppellaro, K. K. Andersson, K. L. Bren, *Inorg. Chem.* 2011, **50,** 12018-12024.

27. J. D. Bryngelson, J. N. Onuchic, N. D. Socci, P. G. Wolynes, *Proteins: Struct., Funct., Genet.* 1995, **21,** 167-195.

28. J. D. Bryngelson, P. G. Wolynes, *Proc. Natl. Acad. Sci. USA* 1987, **84,** 7524-7528.

29. W. Colón, L. P. Wakem, F. Sherman, H. Roder, *Biochemistry* 1997, **36,** 12535-12541.

30. S. J. Hagen, R. F. Latypov, D. A. Dolgikh, H. Roder, *Biochemistry* 2002, **41,** 1372-1380.

31. E. V. Pletneva, H. B. Gray, J. R. Winkler, *Proc. Natl. Acad. Sci. USA* 2005, **102,** 18397-18402.

32. C. Struvay, G. Feller, *Int. J. Mol. Sci.* 2012, **13,** 11643-11665.

33. E. J. King, *Acid-Base Equilibria*. Macmillan: New York, 1965; pp 184-217.

34. D. D. Perrin, B. Dempsey, *Buffers for pH and Metal Ion Control*. Chapman and Hall: London, 1974.

35. J. J. Christensen, L. D. Hansen, R. M. Izatt, *Handbook of Proton Ionization Heats and Related Thermodynamic Quantities*. John Wiley & Sons: New York, 1976.

36. S. P. Datta, A. K. Grzybowski, *J. Chem. Soc. B* 1966, 136-140.

37. E. F. Pettersen, T. D. Goddard, C. C. Huang, G. S. Couch, D. M. Greenblatt, E. C. Meng, T. E. Ferrin, *J. Comput. Chem.* 2004, **25,** 1605-12.

38. D. Ringe, G. A. Petsko, *Meth. Enzymol.* 1986, **131,** 389-433.

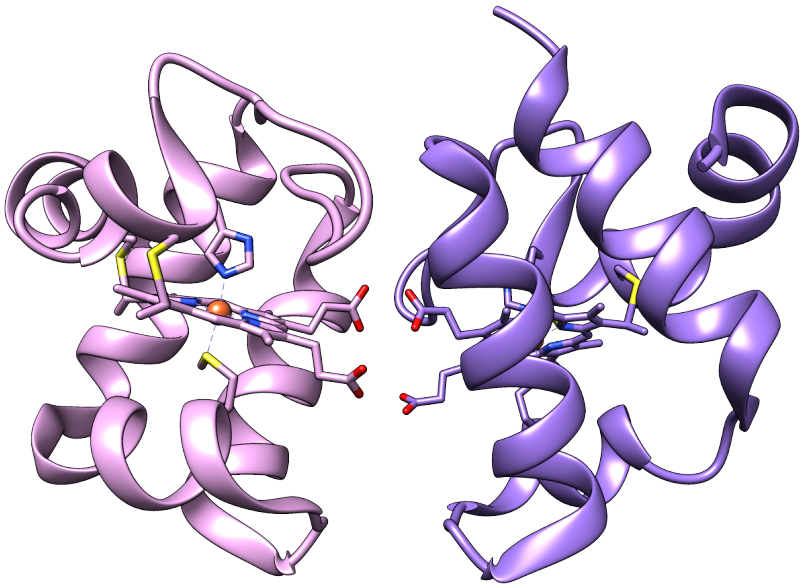

Figure 1. Molecular structure of one dimer unit of *Cp*cyt c_{552}, showing the heme covalently bound to Cys14 and Cys17 and the heme iron axially coordinated to His18 and Met57. (PDB: 4O1W)

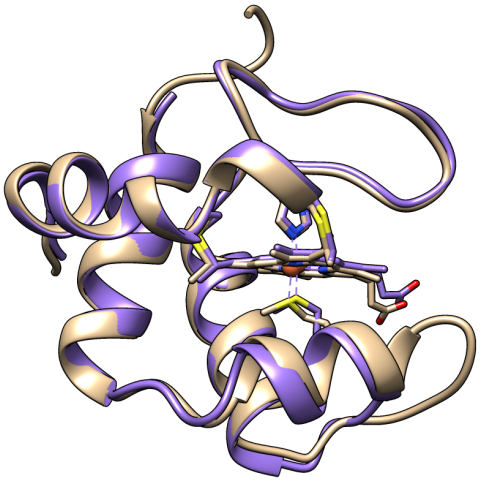

Figure 2. One monomer (chain B) of *Cp*cyt c_{552} (purple, PDB: 4O1W) superposed with one monomer (chain A) of *Mh*cyt c_{552} (tan, PDB: 1CNO).

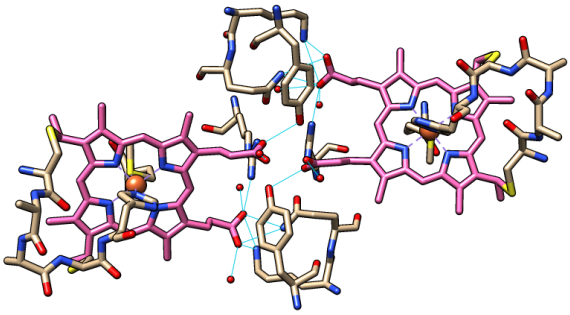

Figure 3. *Cp*cyt c_{552} dimer interface, showing hydrogen-bonding interactions between the heme propionates, waters of crystallization, and Tyr39, Lys42, Gln43, and Arg52.

Table S1. Crystallographic Data Collection and Refinement
(Data in parentheses are for the highest resolution shell)

Wavelength (Å)	0.97950
Resolution range (Å)	19.95 - 2.002 (2.073 - 2.002)
Space group	C 1 2 1
Unit cell	a = 130.28, b = 45.043, c = 87.574
	$\alpha = 90$ $\beta = 90.85$ $\gamma = 90$
Total reflections	
Unique reflections	34186 (3176)
Multiplicity	3.49
Completeness (%)	98.64 (93.19)
Mean I/sigma(I)	11.69 (6.39)
Wilson B-factor	23.44
R-merge	0.108
R-work	0.1701 (0.1662)
R-free	0.2171 (0.2121)
Number of atoms	7440
macromolecules	3393
ligands	277
water	204
Protein residues	477
RMS(bonds)	0.015
RMS(angles)	1.53
Ramachandran favored (%)	99
Ramachandran outliers (%)	0
Clashscore	8.71
Average B-factor	25.20
macromolecules	25.40
ligands	19.30
solvent	29.20

```
         10         20         30         40         50
 GDAAAGKAK SVMCAACHGA AGVSAVPTYP NLAGQKEAYL TKQLNDFKSG

         60         70         80         90        100
KRNDPTMKGM VMALSPADME NLAAYYANMK PGTKMIFAGI KKKTEREDLI

       109
AYLKKATNE
```

Figure S1. Amino acid sequence of cytochrome c_{552} from *Colwellia psychrerythraea*, numbered to be consistent with cyt c_{552} from *Marinobacter hydrocarbonoclasticus*. Labeled in bold are the covalent heme attachments (Cys14 and Cys17) and the native axial metal-binding residues (His18 and Met57).

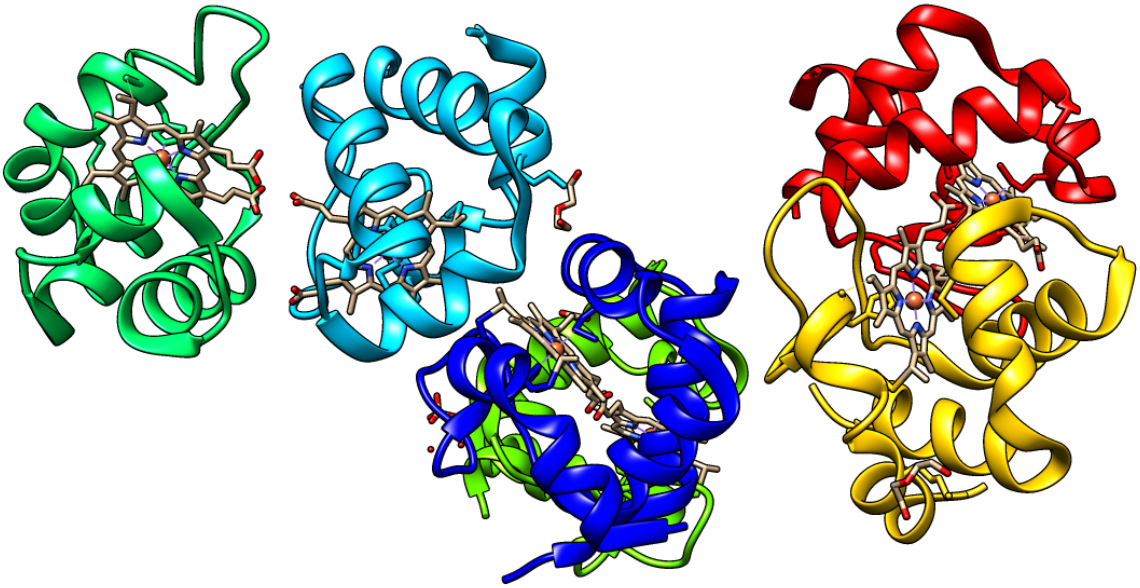

Figure S2. Molecular structure of *Cp*cyt c_{552} showing the three dimer pairs in the asymmetric unit.

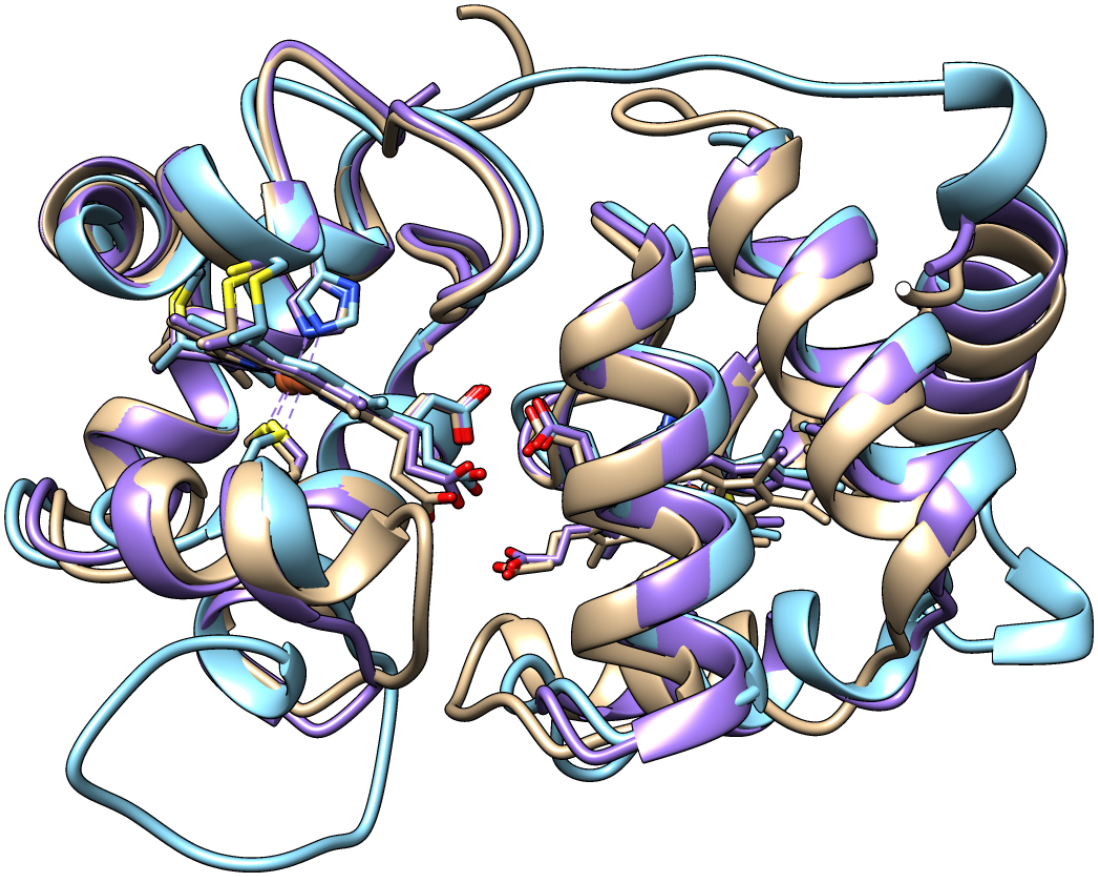

Figure S3. Superposition of the structures of a *Cp*cyt c_{552} dimer (4O1W, purple), a *Mh*cyt c_{552} dimer (1CNO, tan), and the two-heme cyt c_4 from *Pseudomonas stutzerii* (1ETP, blue).

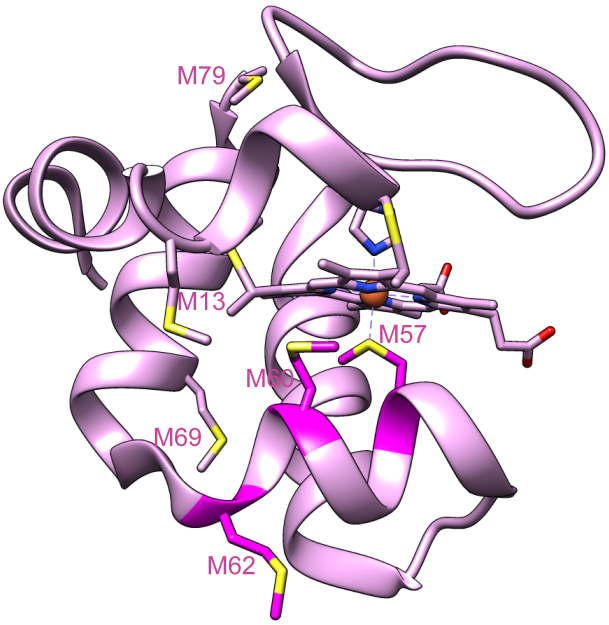

Figure S4. Structure of *Cp*cyt c_{552} monomer showing the position of the six methionine residues. Met57 (the axial methionine), Met60, and Met 62 are shown in darker magenta and are highly conserved in psychrophilic cytochromes. Met13, Met69, and Met79 are shown in lighter pink and are conserved as hydrophobic amino acids but not specifically as methionine.

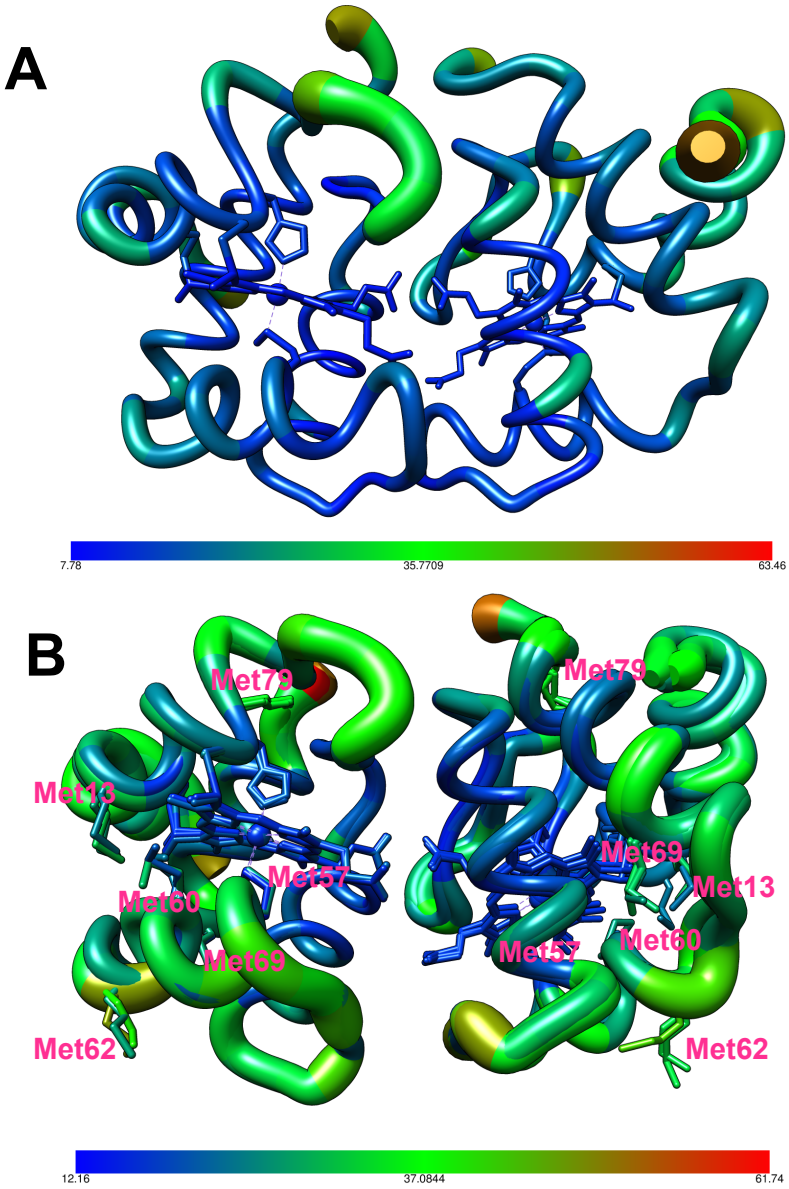

Figure S5. Structures of cyt c_{552} colored by residue-averaged B-factor. The structures are depicted using "worms," with the diameter of the "worm" proportional to the B-factor. The greater average B-factors for the *Cp*cyt c_{552} (**B**) structure, particularly in the outer portions of the structure, are consistent with greater flexibility and dynamics than observed for the *Mh*cyt c_{552} structure (**A**).

A. Structure of *Mh*cyt c_{552} (PDB: 1CNO) **B**. Structure of *Cp*cyt c_{552} (PDB: 4O1W). The three dimers found in the asymmetric unit are superposed. Methionine residues are highlighted. Met62 in particular exhibits relatively high B-factors, consistent with high flexibility or dynamics.

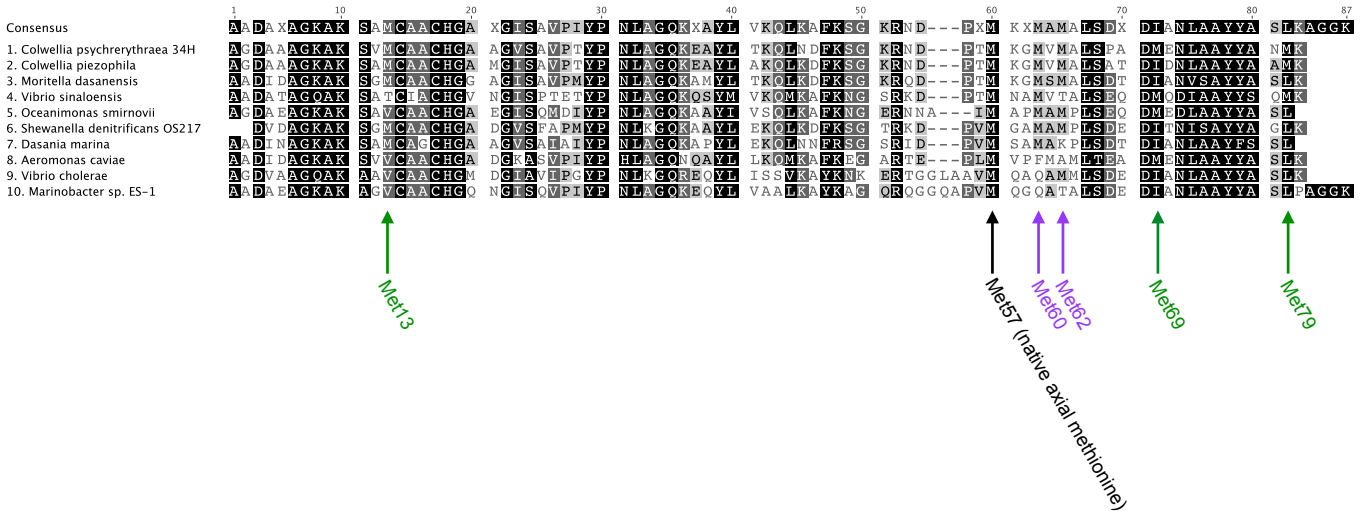

Figure S6. Sequence alignment of ten homologous cytochrome *c* sequences. Sequences 1-3 are from psychrophiles, sequences 4-7 are from psychrotolerant species, and sequences 8-10 are from mesophiles. Met60 and Met62 are highly conserved as methionines in psychrophiles, fairly well-conserved in psychrotolerant species, and not well-conserved in mesophiles. Met13, Met69 and Met79 are well conserved as hydrophobic residues (*e.g.*, Met, Ile, Leu, Val) but not necessarily as methionine. The trends exemplified here are also observed in a larger sequence alignment that includes the top 100 sequences from a BLAST search of *Cp*cyt c_{552} against the NCBI nr protein database.

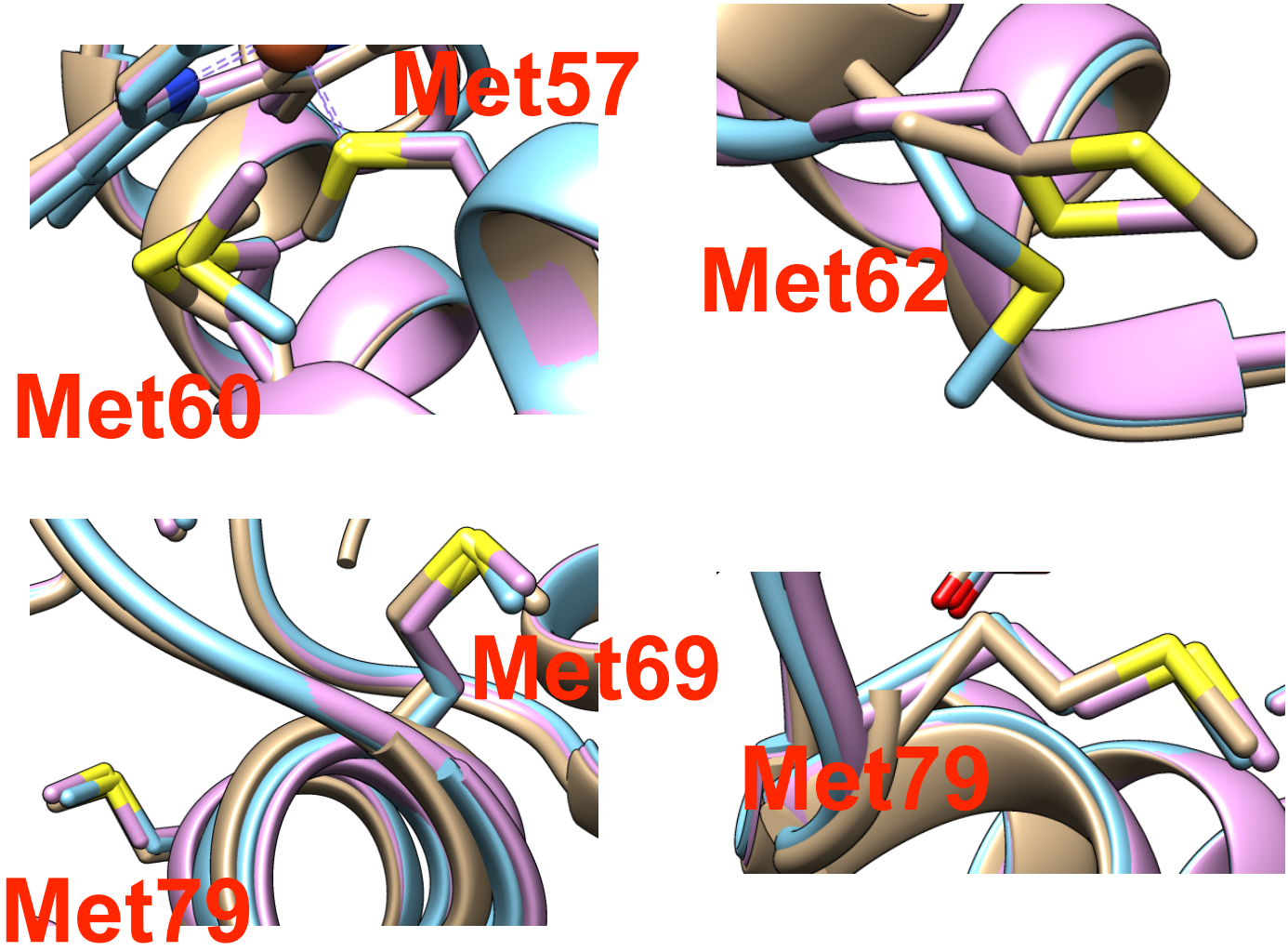

Figure S7. Superposition of the three dimers found in the *Cp*cyt *c*552 asymmetric unit highlighting the methionine residues, with chain A in purple, chain C in blue, and chain E in tan. There are substantial differences in the positions of Met60 and Met62 in each of the three chains. By contrast, Met69, Met79, and Met57 (the axial methionine) from each chain are highly superposable.

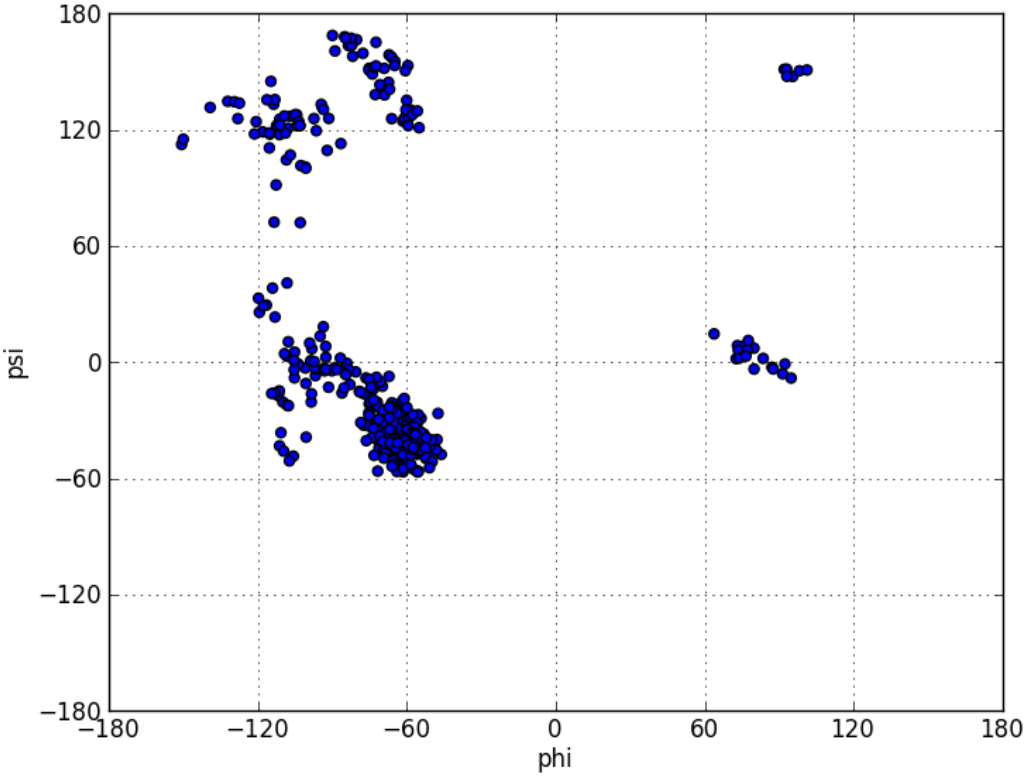

Figure S8. Ramachandran plot for *Cp*cyt c_{552}.